Available online at www.sciencedirect.com
SCIENCE DIRECT
Microporous and Mesoporous Materials 87 (2006) 243–254
MICROPOROUS AND MESOPOROUS MATERIALS
www.elsevier.com/locate/micromeso

Structural and physicochemical properties of natural zeolites: clinoptilolite and mordenite

O. Korkuna [a,*], R. Leboda [b], J. Skubiszewska-Zięba [b], T. Vrublevs'ka [a], V.M. Gun'ko [c], J. Ryczkowski [b]

[a] *Analytical Chemistry Department, Ivan Franko National University of L'viv, Kyrylo and Methodij Str, 6, 79005 L'viv, Ukraine*
[b] *Faculty of Chemistry, Maria Curie-Sklodowska University, Maria Curie-Sklodowska Sq.3, 20-031 Lublin, Poland*
[c] *Institute of Surface Chemistry, 17 General Naumov Street, 03164 Kiev, Ukraine*

Received 31 March 2004; received in revised form 20 May 2005; accepted 20 May 2005
Available online 6 October 2005

Abstract

Natural, H-form and Pd-containing clinoptilolite and mordenite were characterized using adsorption, AFM, FTIR, and TG–DTA methods. The initial natural adsorbents have small specific surface area which increases significantly after their modification. FTIR spectra show the presence of the same typical bands in natural and H-form zeolites. However, the spectra of Pd-including clinoptilolite have a band of ammonia at $v = 1449\ cm^{-1}$, which can be associated with its adsorption complexes with palladium. The TG data show the presence of several types of water, and larger amounts of water desorb from H-forms of both zeolites up to 120 °C that can be caused by stronger changes in the zeolite structure. However, the zeolite skeleton does not change after acidic processing. The changes are more visible for treated clinoptilolite.

Keywords: Clinoptilolite; Mordenite; H-form; Palladium sorption; Porous structure

1. Introduction

Investigations carried out during last years have indicated potential possibilities of application of natural zeolites for concentration and separation of non-ferrous metal ions. Their non-swelling, chemical stability in various caustic media, thermostability and possibility of regeneration as well as a high rate of sorption equilibrium are advantageous. These features of natural zeolites promote their use in the environment protection chemistry and industry [1,2].

Natural clinoptilolites and mordenites from various deposits in Japan [3,4], USA [5], Italy [6,7], Greece [8], South Africa [9], Bulgaria [10], and Ukraine [11–20] are used for the concentration of Cd(II), Cr(III), Cu(II), Fe(II), Mn(II), Ni(II), Pb(II), Zn(II), Sr(II), and NH_4^+. Modified zeolites from Mexico are also used for anion sorption, in particular CrO_4^{2-} and F^- [21,22]. Additionally, they were applied for waste disinfections [23]. Platinum metal ions are often present, though in small amounts, in wastes of jewelry and electrical engineering production; therefore, previous concentration should be maintained both for their determination and utilization using such adsorbents as zeolites. Zeolites are also used as catalysts [2,24–26] whose properties can be improved by incorporation of certain metals into the zeolite structure. Palladium which is one of such metals is a catalyst of many organic and inorganic syntheses [27,28].

The aim of this paper is to study the sorption properties of natural Transcarpathian zeolites such as clinoptilolite and mordenite and their acid modified forms for the concentration of Pd(II). The beds of these zeolites in the Transcarpathian region are more than 1 billion tons, and their application is cheaper than synthetic sorbents. In

* Corresponding author.
E-mail address: okorkuna@pisem.net (O. Korkuna).

1387-1811/$ - see front matter © 2005 Elsevier Inc. All rights reserved.
doi:10.1016/j.micromeso.2005.08.002

our previous papers [29–33] the influence of several factors on the Pd(II) sorption was studied in the static regime: pH of medium, sorbent grain sizes, effect of matrix ions, particularly of mineral salts concentration, time of sorption equilibrium, and thermal treatment. The optimum conditions of sorbent H-form preparation have been established. However, for finding out the sorption mechanism it is necessary to investigate the structure as well as physical and chemical properties of both initial and modified sorbents. Therefore, another aim of this paper is to investigate thermal, structural and spectral properties of natural clinoptilolite and mordenite, their H-forms and Pd-containing samples.

2. Experimental

2.1. Materials

The clinoptilolite was employed from the beds at Sokyrnytsa (Ukrainian Transcarpathian region). The general formula of Transcarpathian clinoptilolite [34] is: $(K_{2.3}Na_{0.5}Ca_{2.1}Mg_{0.6}Fe(III)_{0.9}Fe(II)_{0.2}Ti_{0.2}) \times (Si_{31.4}Al_{6.5}O_{44}) \times 21.8H_2O$, the chemical composition (in %): SiO_2—67.29; TiO_2—0.26; Al_2O_3—12.32; Fe_2O_3—1.26; FeO—0.25; MgO—0.29; CaO—3.01; Na_2O—0.66; K_2O—2.76; H_2O—10.90, whereby the content of the main mineral is $85 \pm 6\%$.

Mordenite was employed from the beds at Lipcha (Ukrainian Transcarpathian region). The general formula of Transcarpathian mordenite [35] is: $(K_2Na_{1.5}Ca_2Mg_{0.5}) \times (Si_{35.5}Al_{8.1}O_{45}) \times 26.6H_2O$, chemical composition (in %): SiO_2—64.56; TiO_2—0.23; Al_2O_3—12.02; Fe_2O_3—0.95; FeO—0.83; MnO—0.1; MgO—0.68; CaO—3.58; Na_2O—0.94; K_2O—2.03; P_2O_5—0.07; H_2O—13.77. Accordingly to [35] the content of the main mineral is $72 \pm 6\%$.

Fractions of clinoptilolite at the particle size $d_s = 0.355$–0.5 mm and mordenite at $d_s = 0.2$–0.315 mm were chosen for the investigations. Sorbents were washed by distilled water and dried out in air and then at 120 °C for 2.5 h. There were investigated four forms of two kinds of zeolite samples: natural, H-forms (acid treated) and two Pd-forms prepared by the adsorption of Pd(II) ions on natural and acid-treated clinoptilolite and mordenite. The H-forms were prepared by means of acidic modification under static conditions for 24 h. Natural clinoptilolite was treated with 12.0 M HCl solution. Natural mordenite was treated with 3.0 M $HClO_4$ solution. After modification the acid solutions were poured out and the sorbents were well washed by distilled water up to pH about 5.5–6.0, then the sorbents were dried in air.

To prepare Pd-containing samples of natural and H-form clinoptilolite, the Pd(II) sorption from the ammonium solutions at $C_{Pd(II)} = 2.61 \times 10^{-4}$ M and pH 11.5 was carried out. In this case the Pd(II) solution was prepared by dilution of aliquot of the initial Pd(II) solution with 15 ml of 25% ammonia to full volume of 250 ml by distilled water. The initial solution was obtained by dissolving the pure metal (99.99 wt.%) in nitric acid (1:1). Sorbents in the amount of 2 g were added to the Pd(II) ammonium solutions. The palladium adsorption was carried out at 20 °C while shaking for 2.5 h.

For preparing Pd-containing samples of natural and H-form mordenite, the Pd(II) adsorption was carried out from the nitrate solutions at $C_{Pd(II)} = 1.19 \times 10^{-4}$ M and pH 4.0. In this case the Pd(II) solution was prepared by dilution of aliquot of the initial Pd(II) solution to full volume of 250 ml with distilled water. The pH value of the palladium solution was controlled by addition of HNO_3 or NaOH solutions. Sorbents (2 g) were added into nitrate Pd(II) solutions. The palladium adsorption was carried out at 20 °C while shaking for 2.5 h.

After sorption, the sorbent was separated from the residual liquid and washed by distilled water and dried in air. The contents of sorbed palladium were determined by pulse voltammetry using a linearly varying potential (PO-5122 model 03 oscillopolarograph) from the difference between initial and equilibrium Pd(II) concentrations, which remained in the solutions after sorption. For that purpose 20.0 ml of Pd(II) solution were pipetted and 5.0 ml of concentrated $NH_3 \times H_2O$ (pH 11.5) were poured into it as the background electrolyte. Palladium(II) is reduced using 1 M NH_4OH + 1 M NH_4Cl as a background electrolyte at a potential of −0.720 V saturated calomel electrode (SCE). A temperature-controlled two-electrode cell (22 ± 0.5 °C) with an indicator mercury dropping electrode and a SCE were employed for such measurements; the capillary characteristics were as follows: $m = 0.789$ mg s^{-1} and $\tau = 9.48$ s. Peak potentials were measured directly at the maximum point of the polarogram using a V7-21 voltammeter with the precision ±1 mV. The solution was purified from oxygen by blowing hydrogen obtained by means of electrolysis. The pH value was controlled using a pH-573 apparatus with saturated silver chloride comparable electrode. Polarographic determination was carried out in the following regime of oscillopolarograph work: $E_{init} = -0.300$ V, velocity of polarized potential $v = 0.5$ V/s, and $\tau_{ret} = 5$ s. Pd(II) determination was made from comparative measurements using a standard addition method. Average palladium contents in the samples are shown in Table 1.

2.2. Adsorbents testing

2.2.1. Nitrogen adsorption

The low-temperature nitrogen adsorption/desorption isotherms (77.4 K) were recorded using an ASAP 2010 (Micromeritics, Norcross, GA, USA) adsorption analyzer. The specific surface area S_{BET} was calculated according to the standard Brunauer–Emmet–Teller (BET) method. The total sorption pore volume V_p (estimated at $p/p_0 \approx 0.98$, where p and p_0 denote the equilibrium and saturation pressures of nitrogen, respectively), and the mean pore radius $R_p = 2V_p/S_{BET}$ (assuming a cylindrical shape of pores) were calculated from the adsorption data.

Table 1
Palladium (II) content in zeolite samples

Sample	C_{Pd}, mg/g
Pd–Nat-clin	0.8960
Pd–H-clin	9.5318
Pd–Nat-mord	0.3750
Pd–H-mord	5.7629

The pore size distributions (PSDs) (differential PSD $f_V(R) \sim dV_p/dR$) of the studied minerals were calculated using modified overall adsorption equation in the form proposed by Nguyen and Do (ND method) for slit-like pores [36,37] and modified for cylindrical pores [38–40]. The nitrogen desorption data were utilized to compute the $f_V(R)$ distribution functions using the modified regularization procedure CONTIN [41] under non-negativity condition ($f_V(R) \geqslant 0$ at any R) with a fixed regularization parameter $\alpha = 0.01$. The $f_V(R)$ distribution functions linked to the pore volume can be transformed to the distribution functions $f_S(R)$ with respect to the specific surface area using the corresponding models of pores

$$f_S(R) = \frac{w}{R}\left(f_V(R) - \frac{V_p}{R}\right), \quad (1)$$

where $w = 2$ for cylindrical pores. For pictorial presentation the pore size distribution functions were calculated as incremental PSDs (IPSDs)

$$f_{x,n}(R_i) = 0.5(f_x(R_i) + f_x(R_{i-1}))(R_i - R_{i-1}), \quad (2)$$

where subscript $x = V$ or S.

2.2.2. Electron microscopy

Atomic force microscopic (AFM) images were obtained by means of a NanoScope III (Digital Instruments, USA) apparatus using a tapping mode AFM measurement technique. Before AFM scanning, powder samples of sorbents were slightly smoothed by hand pressing using a glass plate.

2.2.3. X-ray analysis

The specimens of zeolites were examined by an X-ray powder diffraction technique HzG 4A2 (GDR) using CuKα radiation, $\theta/2\theta$-scanning mode, 0.03° step size, 8 s step time and measurement range of 5–40°. The obtained patterns were compared with the JCPDS-ISDD files.

2.2.4. FTIR photoacoustic spectroscopy

Spectral data were collected by a Bio-Rad Excalibur 3000MX FT-IR spectrometer and a helium-purged MTEC 300 photoacoustic cell. All the spectra were recorded over the 4000–400 cm^{-1} region at a spectral resolution of 8 cm^{-1} and with the 1024 scans co-added. The spectra were normalized proportioning the sample spectrum with a carbon black spectrum.

2.2.5. Thermogravimetric analysis

The thermal behavior of zeolites was investigated in the temperature range 20–1000 °C using a Derivatograph C (Paulik, Paulik, and Erdey, MOM, Budapest) with a linear heating rate of 10 °C/min. The analysis was conducted in air using platinum crucibles and employing Al_2O_3 as a reference standard. The measurement errors were ±5%.

3. Results and discussion

Clinoptilolite and mordenite are aluminium silicates with high silica contents. The crystal structure of clinoptilolite has 2D view channels, formed by tetrahedra layers. Channels A (10-member rings, free diameters 0.44 × 0.72 nm) and B (8-member rings, free diameters 0.41 × 0.47 nm) are parallel to each other, while C channels (8-member rings, free diameters 0.40 × 0.55 nm) intersect both A and B channels. The elliptitic-shaped 8- and 10-member rings that form the channel system are non-planar [42,43].

The crystal structure of mordenite is very complicated. Mordenite contains two different types of pore channels and void systems. Channels A are formed by the assemblage of 12-membered rings, each of which has 12 oxygen atoms. Channels B are in the turn made of 8-membered rings in which there are 8 oxygen atoms. Channels A are elliptical, with free diameters 0.65 × 0.70 nm, while free diameters of the 8-membered rings are 0.26 × 0.57 nm. Channels A and B are interconnected via the perpendicular channel B tubes, in the form of small side pockets [4,35].

Zeolites are microporous materials with voids smaller than 2 nm in diameter. Micropores can be subdivided into ultramicropores (pore width less than 0.7 nm) and supermicropores (pore width between 0.7 and 2 nm). The zeolite pore space is filled in a volumetric manner rather than a layer-by-layer mechanism because of proximity of the surrounding pore walls to the adsorbate molecules. The sorption uptake increases with pressure; saturation of each pore domain with adsorbate molecules depends not only on the size and shape of the microporous channels and cavities, but also on the size and geometry of the adsorbate molecules [42]. With respect to the filling of micropores with adsorbate molecules in the lower relative pressure region, two different adsorptive processes take place, i.e. a primary process develops from very low relative pressures up to a value of ~0.01. This process is assumed to occur in the ultramicropores and involves the accommodation of one or two layers of molecules. The secondary process takes place in the supermicropores at relative pressures between 0.01 and 0.1, where up to five layers of adsorbed nitrogen molecules can be accommodated. Next the cavities are filled by means of molecular condensation. More detailed mechanism of pore filling is described in [42,43].

The adsorption–desorption isotherms for certain clinoptilolite and mordenite samples are shown in Figs. 1 and 2. Based on conventional classification of adsorption isotherms, all measured isotherms can be considered as

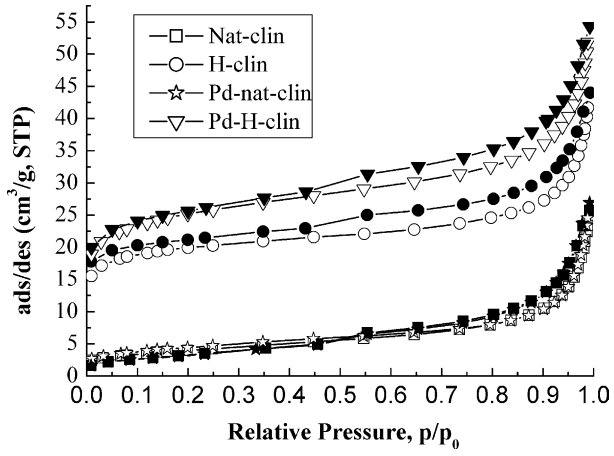

Fig. 1. Low temperature adsorption/desorption isotherms of nitrogen on the clinoptilolite (empty symbols—adsorption and full symbols—desorption).

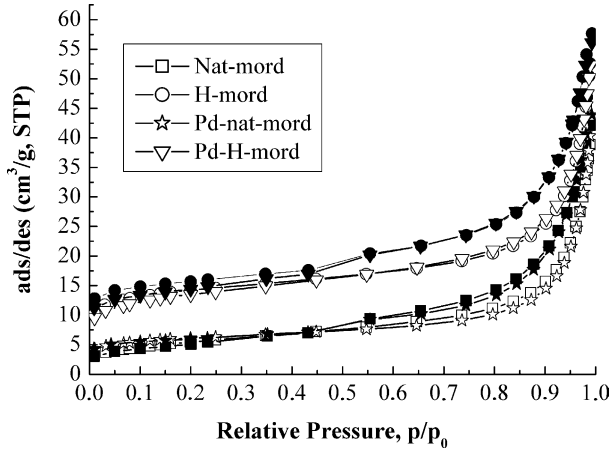

Fig. 2. Low temperature adsorption/desorption isotherms of nitrogen on the mordenite (empty symbols—adsorption and full symbols—desorption).

isotherms of IV type. The hysteresis loops are typical of mesoporous materials with flat slits between two crystalline planes, according to the clinoptilolite structure [12,15]. As follows from Fig. 1, the boundary ascending curve of the Nat-clin isotherm with narrow high-pressure hysteresis loop is akin to a standard nitrogen isotherm on a non-porous substrate. Ions (e.g. Na^+, K^+, Ca^{2+}) located in narrow zeolite channels make barriers for nitrogen molecules diffusion. Therefore contribution of narrow pores to PSD is insignificant (Fig. 3). The natural substratum also allows for the presence of small amounts of impurities, especially clays, quartz and a macroporous glassy material [35]. In fact the *t*-plot increases very slowly along a wide range of relative pressures and the BET surface area is small (14 m^2/g). The H-clin isotherm presents a very wide and open hysteresis loop over the whole pressure range. The low-pressure hysteresis may indicate the increased complexity of zeolite channels after acid treatment. As a whole, acid treatment of the natural clinoptilolite improves the adsorbent characteristics due to decationation and dealumination, and also by dissolving amorphous silica fragments blocking the channels. The blocking effect by cations in the treated clinoptilolite is decreased because contribution of micropores increases significantly (Fig. 3). Eventually a continued acid treatment also diminishes further cation exchange by leaching Al^{3+} from framework positions while introducing H^+ into a few remaining cation locations. The isotherms of Pd-containing samples are similar to those of Nat-clin and H-clin. The nitrogen isotherms for the mordenite samples (Fig. 2) are akin to those of the clinoptilolite samples (Fig. 1), and also changes in the texture occurring due to different treatment procedures. All samples have three kinds of pores including narrow pores with the radius $R < 2$ nm, between 2 and 5 nm and $R > 5$ nm. All the treatments change mainly narrow pores at $R < 5$ nm. Broader pores are less sensitive to these treatments. Consequently, the zeolite skeleton remains almost unchanged.

Table 2 presents the parameters of porous structure of various clinoptilolite and mordenite forms. As follows from the data in Table 2, the studied sorbents are characterized by small specific surface area which increases significantly after acid treatment of both clinoptilolite by 6.5 times and mordenite by 2.6 times, respectively. From papers [12,14,42,43] for natural clinoptilolite, regardless of deposit, the value S_{BET} is inherent in the range of 11–16 m^2/g, but natural mordenite is characterized by $S_{BET} = 115$–120 m^2/g [13,42]. In our case the S_{BET} value for clinoptilolite is 14 m^2/g that is correlated with the literature data; however, for mordenite it is considerably lower, only 19 m^2/g. This can testify the presence of other minerals (e.g. clinoptilolite) in mordenite deposits.

In accordance with [14,42,43] repeated treatment of the sorbent by the dilute acid gives better results than single treatment by the concentrated acid. So, in the case of a single acid treatment of clinoptilolite with 2 M HCl, its S_{BET} value grows from 16 to 97 m^2/g, and repeated treatment changes it from 11 to 160 m^2/g. In our case the treatment was single, that experimental data are presented. Besides, acid treatment led to diminishing average pore radii of natural clinoptilolite by 3.5 times, and natural mordenite by 2.5 times.

The samples of natural zeolites do not possess microporous structure, which, however, is observed for hydrogen forms of clinoptilolite and mordenite. It should be stated that the mesopores structure (at $R > 5$ nm) does not change due to palladium sorption because pore volume is not changed in the samples with palladium, except Pd–H-clin. Here it is necessary to take into account that the effective diameter of $[Pd(NH_3)_4]^{2+}$ sorbed on H-clin is ~0.8 nm, however, the average pore diameter of H-clin is 3.4 nm, which is much larger than the size of sorbed $[Pd(NH_3)_4]^{2+}$ ion. The average pore diameter of Nat-clin is 9.0 nm. Therefore, it is possible to assume that already at such correlation of ion and H-clin channel sizes, a sieve mechanism can occur in the sorption process. In the case of Pd-con-

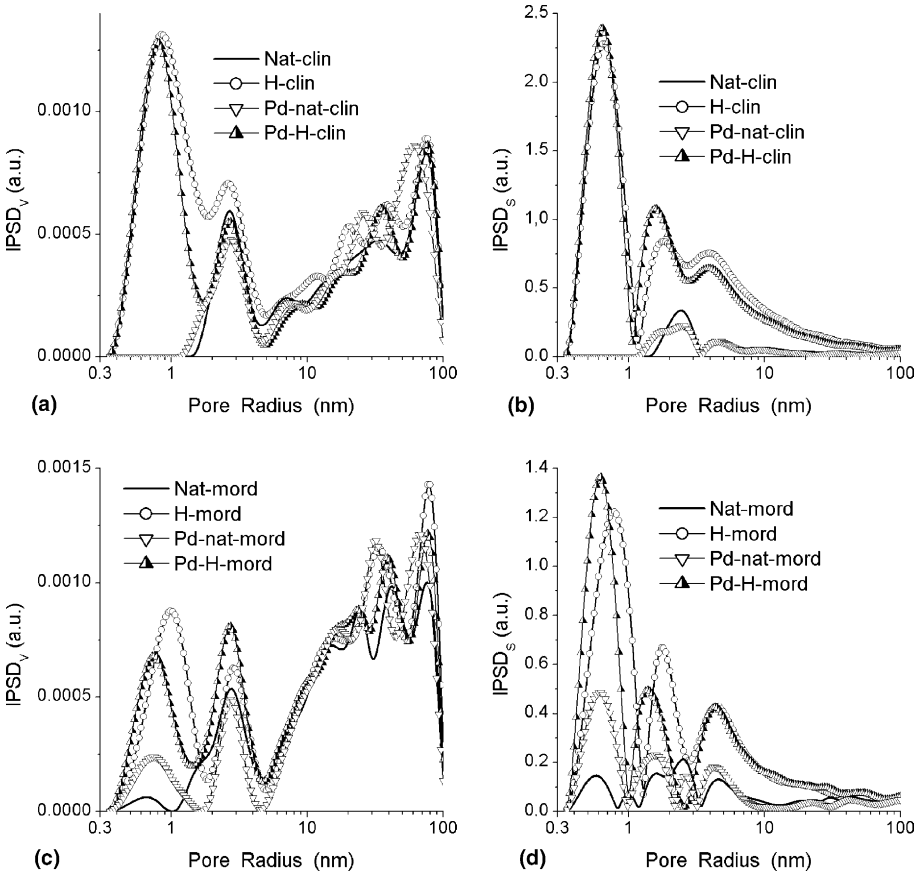

Fig. 3. Incremental (a, c) PSD$_V$ and (b, d) PSD$_S$ for (a, b) clinoptililite and (c, d) mordenite samples.

Table 2
Structural characteristics of studied sorbent forms

Sample	S_{BET}, m^2/g	V_p, cm^3/g	V_{mic}, cm^3/g	V_{mes}, cm^3/g	V_{mac}, cm^3/g	S_{mic}, m^2/g	S_{mes}, m^2/g	S_{mac}, m^2/g	R_p, nm
Nat-clin	14	0.032	0	0.022	0.019	0	13	2	4.5
H-clin	89	0.075	0.022	0.040	0.022	42	43	3	1.7
Pd–nat-clin	16	0.033	0	0.021	0.021	0	14	2	4.2
Pd–H-clin	70	0.059	0.022	0.026	0.020	34	34	2	1.7
Nat-mord	19	0.053	0.001	0.035	0.029	4	13	3	5.5
H-mord	50	0.073	0.012	0.041	0.036	23	25	3	2.9
Pd–nat-mord	22	0.055	0.004	0.030	0.034	10	10	2	5.1
Pd–H-mord	48	0.073	0.012	0.042	0.033	24	21	3	3.1

tained samples of mordenite Pd(II) sorbs as $Pd[(H_2O)_{4n}(OH)_n]^{2-n}$ [29] with the effective diameter still smaller than the effective diameter of $[Pd(NH_3)_4]^{2+}$, and diameter of mordenite channels still larger than clinoptilolite (11.0 nm for Nat-mord; 5.8 nm for H-mord). Consequently, in all cases except for H-clin, palladium sorption proceeds only according to the ion-exchange mechanism, because those ions, which do not take part in ion-exchange cannot stay too long inside sorbent channels.

Images obtained by using AFM allow us to see the sorbents structure with different magnification. Sullivan et al. [44] presented low-resolution TMAFM images of natural clinoptilolite, which indicated the presence of monoclinic crystals with excellent crystal faces with small crystal fragments, which adhered to the flat crystal faces and edges. In the present paper the microphotographs of some clinoptilolite (Fig. 4) and mordenite (Fig. 5) samples are well correlated with the literature data. As follows from Fig. 4 after acidic processing the clinoptilolite surface smoothed out, that can be explained by elution of exchange cations and even partly aluminium. However, as a result of the Pd(II) sorption the sorbent surface becomes clearer, which can be connected with recrystallization in alkaline medium, where sorption took place in this case.

As follows from Fig. 5 in the case of Pd–nat-mord there were observed separated fibres, since the sorbent was heterogeneous and sorption took place in the acidic medium. In the case of Pd–H-mord there was observed eroding of

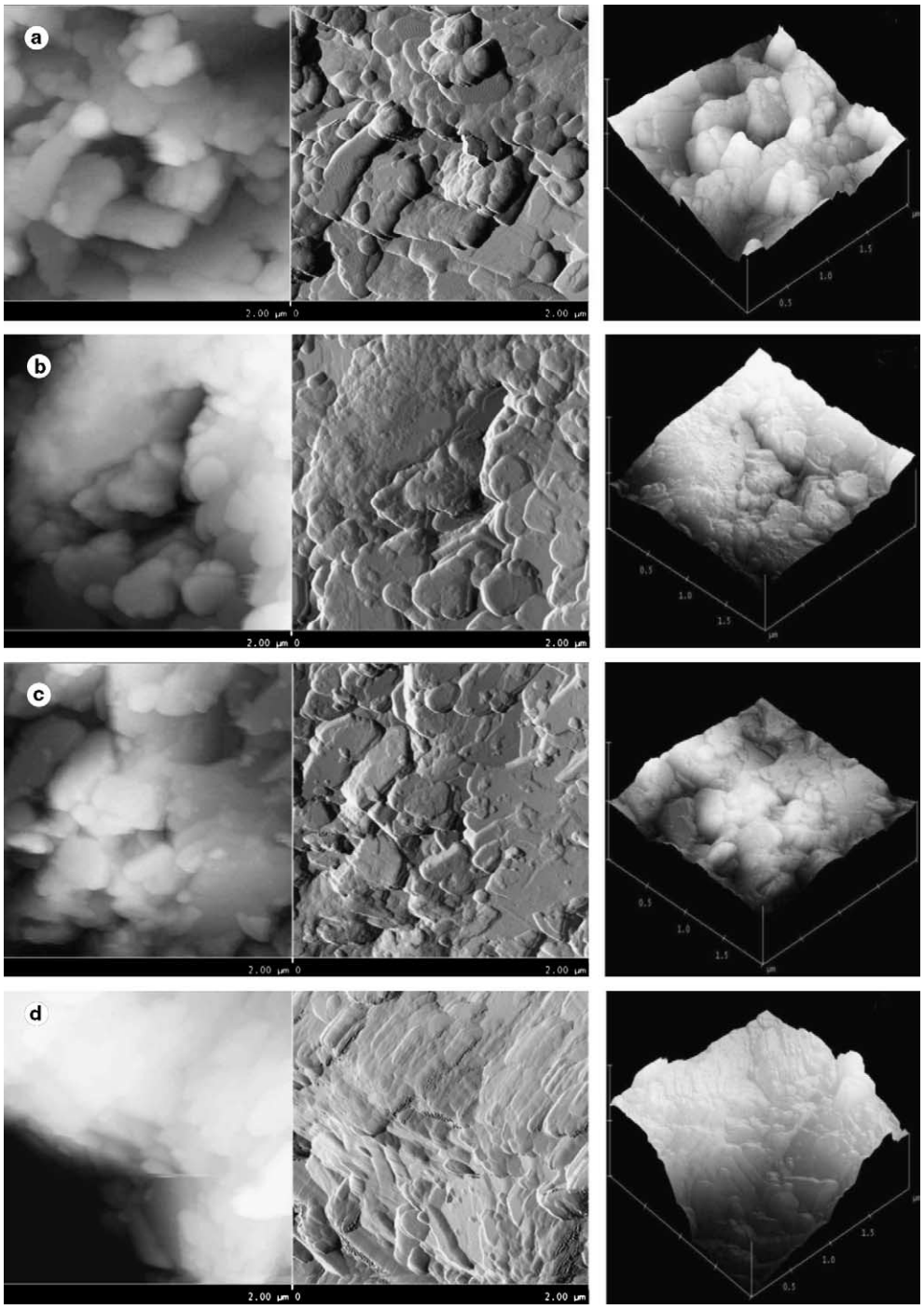

Fig. 4. 2D (1—spatial view; 2—topographical view) and 3D AFM images (1×2 μm) of different forms of clinoptilolite.

surface contour and as a result of this the samples became more homogeneous because they were twice in the acidic medium during modification and during sorption.

X-ray diffraction analysis of the zeolites showed that the positions and intensities of many of the reflections correspond to the literature data for clinoptilolite [3,13,19,20,2223,35,45–47] and mordenite [3,11,27,42,45]. The obtained data (Figs. 6 and 7) indicate an increase of the amorphism in the H-form of both zeolites.

X-ray examination of the clinoptilolite samples showed (Fig. 6) that modification of clinoptilolite with 12.0 M solution of HCl for 24 h does not lead to significant structural changes. The comparative analysis of the powder patterns of both natural and H-form of clinoptilolite showed that there are no detectable changes in the peak positions, although some small peaks disappeared at $2\theta = 22.15°$, $23.54°$, $24.16°$, $26.18°$, and $38.09°$, and the peak at $2\theta = 27.62°$ appeared. Moreover, a decrease of

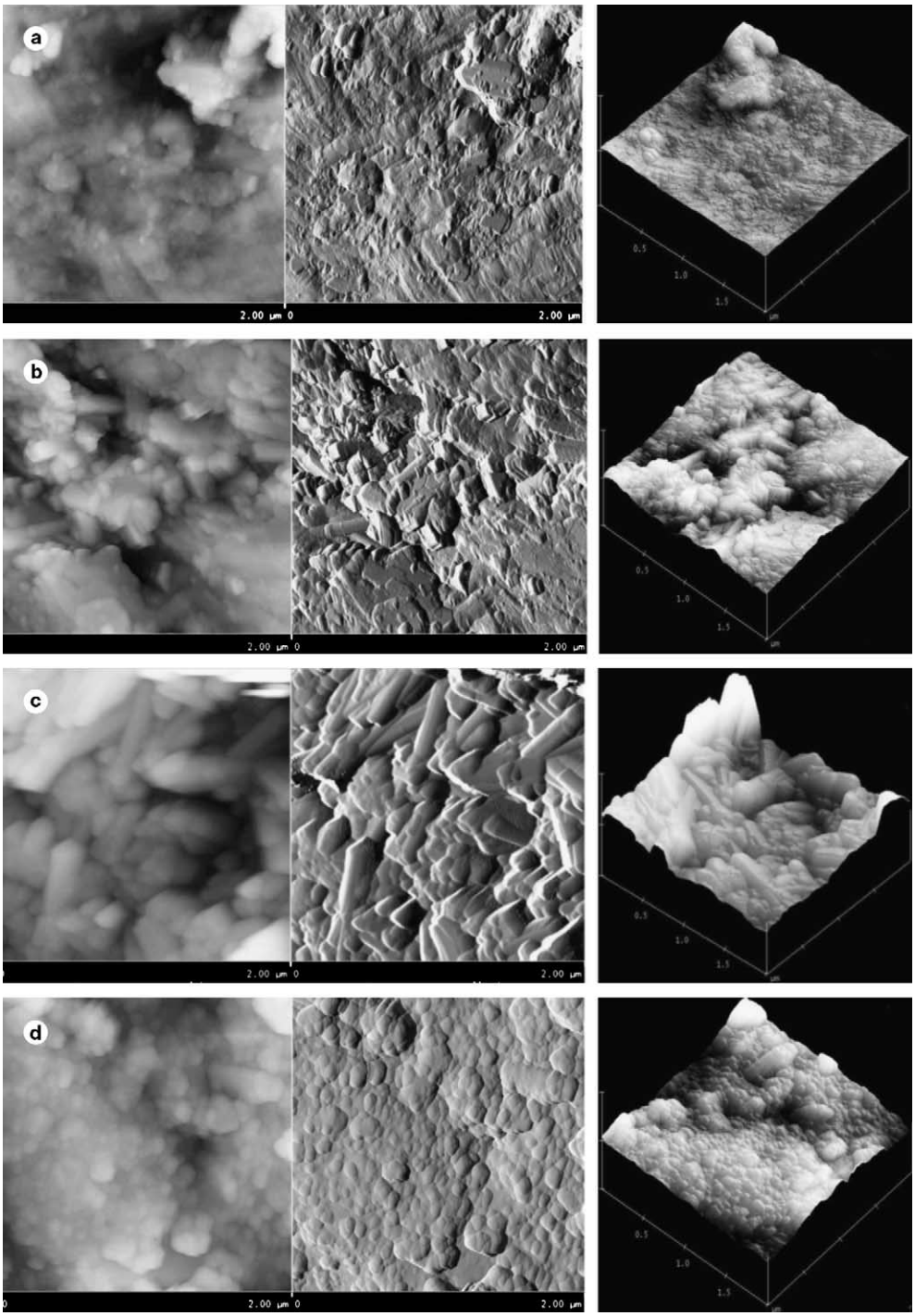

Fig. 5. 2D (1—spatial view; 2—topographical view) and 3D AFM images (1×2 μm) of different form of mordenite.

peak intensities is observed after modification, except for the peak at $2\theta = 26.60°$, which is connected with elimination of admixtures. Vasylechko et al. [20] observed similar changes after treatment of Transcarpathian clinoptilolite with 1.0 M HCl solution. The phase analysis shows that besides reflections of clinoptilolite some peaks of α-quartz are present. In Pd-containing samples of Nat-clin peaks at $2\theta = 24.26°$; 38.09° disappear that is connected with elimination of admixtures in acid as well as in alkali media. The intensity of peaks at $2\theta = 9.77°$, 20.87°, and 25.97° increases. In Pd–H-clin, new peaks at $2\theta = 12.83°$, 24.47°, and 28.16° appear because of the treatment and sorption carried out in the ammonium medium. The intensity of peaks at $2\theta = 20.78°$, 26.03°, and 27.89° increases. Increasing intensities of the mentioned peaks in Pd–nat-clin ($2\theta = 20.87°$, 25.87°) and Pd–H-clin ($2\theta = 20.78°$, 27.89°) can indicate the presence of Pd in clinoptilolite samples.

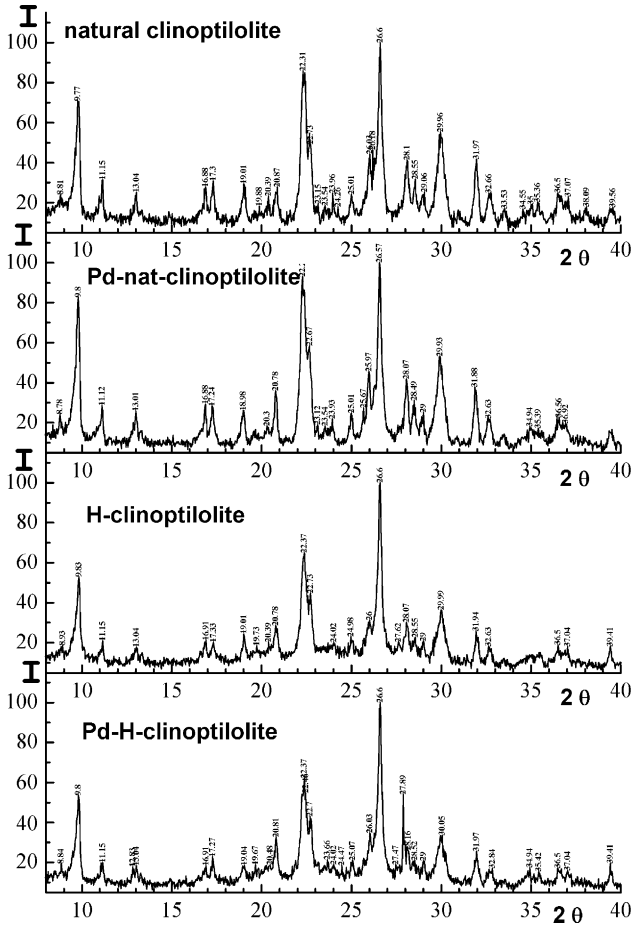

Fig. 6. Powder diffraction patterns of different clinoptilolite forms.

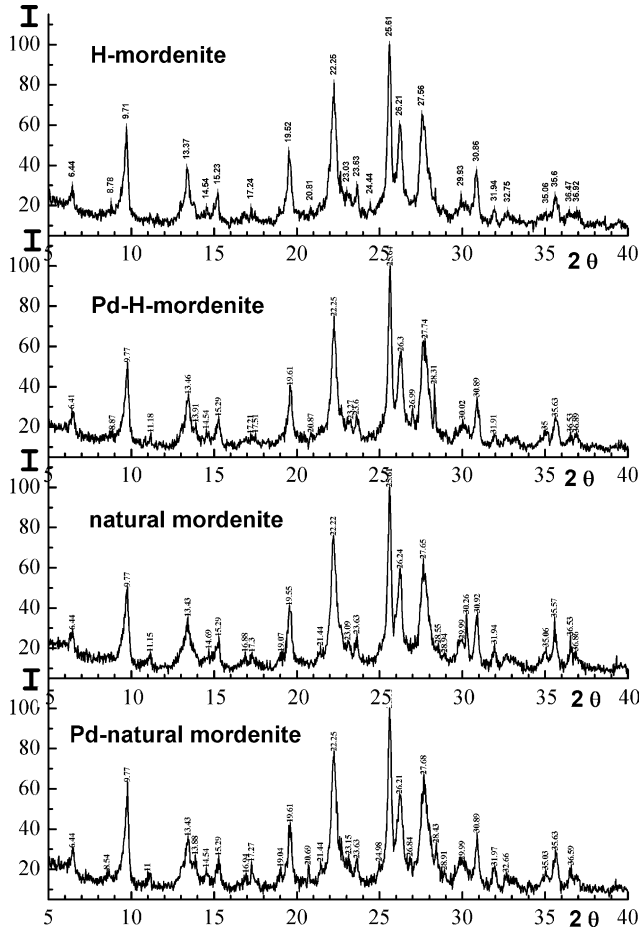

Fig. 7. Powder diffraction patterns of different mordenite forms.

X-ray examination of the mordenite samples shows (Fig. 7) that modification of clinoptilolite with 3.0 M $HClO_4$ solution for 24 h does not lead to significant structural changes. The comparative analysis of the powder patterns of both Nat-mord and H-mord shows that small peaks at $2\theta = 16.88°$, 21.44°, 28.94°, and 30.26° disappear but two peaks at $2\theta = 13.88°$ and 20.81° appear. Patterns of peaks at $2\theta = 14.54°$ and 32.75° become more clear but the intensity of peaks at $2\theta = 31.94°$, 35.57°, 36.53°, and 36.86° decrease. In Pd–nat-mord a peak at $2\theta = 30.26°$ disappears, but some new peaks at $2\theta = 13.88°$, 20.16°, and 26.84° appear, the intensity of peak at $2\theta = 35.63°$ decreases and at $2\theta = 28.43°$ significantly increases. In Pd–H-mord a new peak at $2\theta = 26.99°$ appears, a peak at $2\theta = 13.91°$ becomes clearer and intensity of peak at $2\theta = 28.31°$ increases significantly. In the case of powder pattern analysis, it was noted that the only appearance of peak at $2\theta = 26.84°$ and increasing peak intensity at $2\theta = 28.31°$ may be connected with palladium presence in the mordenite samples. Dams et al. [27] reported the presence of $2\theta = 34°$ signal from PdO and $2\theta = 40°$ and 47° signals from Pd^0 in the powder patterns of 4% Pd-containing mordenite. It was reported [23] that Mexican zeolitic mineral with the highest Ag content showed differences in its diffraction pattern from 29° to 30° in relation to the sodium zeolitic mineral diffraction pattern. In our investigation the palladium content at H-mord was ~0.5%.

There are two groups of frequencies of vibrations in all zeolites: internal vibrations of T–O (considered insensitive to structure) and vibration of external linkages between tetrahedral, due to topology and the mode of structure arrangement [23]. The FTIR band connected with the internal Si–O(Si) and Si–O(Al) vibrations in tetrahedral or alumino- and silico-oxygen bridges lies in the range of 1200–400 cm^{-1}. The bands due to the presence of zeolite water lie in the range of 1600–3700 cm^{-1}. There are several types of zeolitic water. In paper [47] OH groups heterogeneity was established inside different mordenite channels, which concerns with no equivalence of the Si–OH(Al) groups with a different number of aluminum atoms in the $(SiO)_{3-n}(AlO)Si–O(H)–Al(SiO)_3$ bridges. The OH group is less acidic if the number of aluminum atoms increases because Al possesses less electronegativity. The OH-stretching vibrations at 3620 cm^{-1} are inherent for less acidic groups than that at 3605 cm^{-1}. There are bands due to pseudo-lattice vibrations of structural units (500–700 cm^{-1}) and the bands connected with lattice vibrations (below 400 cm^{-1}) [48].

Embedding of non-tetrahedral cations into the aluminosilicate framework can change the IR spectra in the range of pseudolattice vibrations at 700–500 cm^{-1} and lattice vibrations below 400 cm^{-1}. These changes are more often characterized by shifts in the bands of the framework vibrations [21,22]. It was confirmed [28] that the presence of palladium cations in the zeolitic samples can cause compensated shifts in the bands inherent to the Brønsted acidic sites (Si–O(H)–Al) which interact with Pd(II). The loss of Al^{3+} cations during acid modification should cause shifting of the Si–O(Si) and Si–O(Al) stretching bands at 1088 cm^{-1} to higher wavenumbers [47].

Zeolite surfaces were studied using FTIR/PA spectroscopy (Figs. 8 and 9). As follows from the spectra, practically for all forms of sorbents, there is the band at 3620 cm^{-1} connected to acidic hydroxyls Si–O(H)–Al. A band at 3430 cm^{-1} is due to the vibration of the bonds O–H···O. A band at 1630 cm^{-1} is connected to deformation vibration of absorbed water. A band at 1020 cm^{-1} is due to the asymmetric valence vibrations in tetrahedra SiO_4. There is a small displacement ($\Delta\nu = 10\ cm^{-1}$) of the band at 1061 cm^{-1} for H-clin compared to Nat-clin (Fig. 8), which can indicate elution of a portion of Al^{3+} on acid treatment by 12.0 M solution of HCl. For treated mordenite, similar changes in the FTIR/PAS spectra (Fig. 9) are not observed. For Pd-including clinoptilolite, there is ammonia band at 1449 cm^{-1} which can be connected with both sorbed ammonia complexes with palladium or due to interaction with surface acidic hydroxy species.

Water is on the silicate minerals in two forms as intact molecules and as OH groups formed on dissociation of water interacting with metal (Si^{4+}, Al^{3+}, Be^{3+}) and O^{2-} ions. Physically adsorbed water is mainly eliminated at $T < 100$ °C. Hydroxyls are removed through the associative desorption mechanism at ~100–300 °C or higher. Hydroxyls groups leave the surface mainly at 200–500 °C, moreover the isolated OH groups are eliminated at higher temperatures. At $T > 400$ °C almost all OH-groups on the silicate surface are isolated. Transcarpathian clinoptilolite gives three peaks at 100–105 °C, 140–142 °C and 250–260 °C respectively. It prompts the conclusion that there are at least three types of adsorbed water.

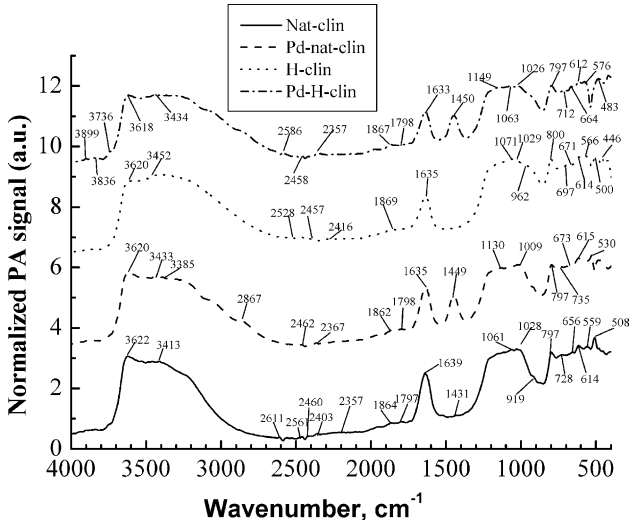

Fig. 8. FT-IR/PAS spectra of clinoptilolite and its modified forms.

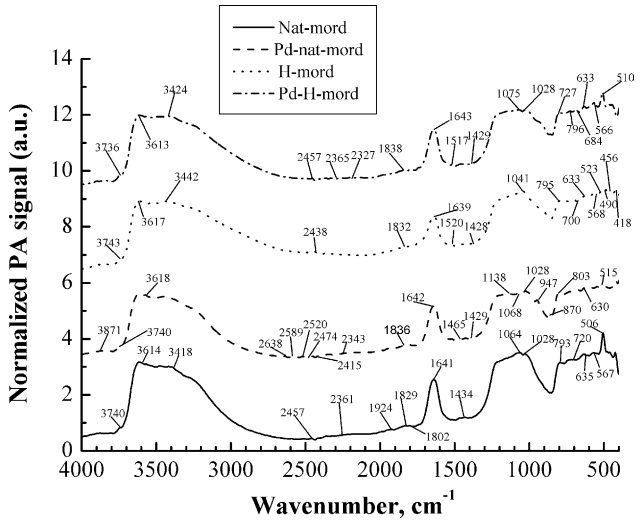

Fig. 9. FT-IR/PAS spectra of mordenite and its modified forms.

The presence of different exchangeable cations in zeolites leads to changes in temperature of zeolitic water elimination, which is held in a few stages [46]. TG curves of some forms of clinoptilolite and mordenite are shown in Figs. 10 and 11, respectively. In the case of H-form of both sorbents, the elimination of intact water is observed up to 120 °C that is caused by complex connectivity of pores and variation in their sizes as a result of exchangeable cation replacement with protons. The presence of palladium in H-clinoptilolite diminishes water content in comparison to clear H-clinoptilolite (Fig. 10). In the case of H-mordenite, a similar effect is not observed (Fig. 11). From the course of DTG curves, it can be seen that temperature of minima (corresponding to the maximal rate of water desorption) depends on the form of a given zeolite.

As follows from DTA curves (Figs. 10 and 11) in the case of both sorbents, endothermic peaks connected with elimination of physically adsorbed water are observed up to 200 °C. However, as follows from Fig. 10, the DTA curves for Pd-containing clinoptilolite reveal exothermic peaks connected with sorbed ammonia complexes. In the case of mordenite, similar peaks are not observed because sorption proceeded in the nitrate medium (Fig. 11).

The results of thermogravimetric analysis of Transcarpathian zeolites (Table 3) testify that thermal treatment of Nat-clin leads to loss of 10.91 wt.% in the range 20–1000 °C because of surface dehydroxylation and dehydratation. Moreover, these processes have an intricate character. The loss is 10.9 wt.% for H-clin, 11.46 wt.% (Pd–nat-clin), and 10.77 wt.% (Pd–H-clin). The loss is 11.8 wt.% for Nat-mord, 13.10 (H-mord), 12.0 (Pd–nat-mord), and 12.62 wt.% (Pd–H-mord). As follows from Table 3 acid treatment and palladium presence do not significantly influence the amount of desorbed water during

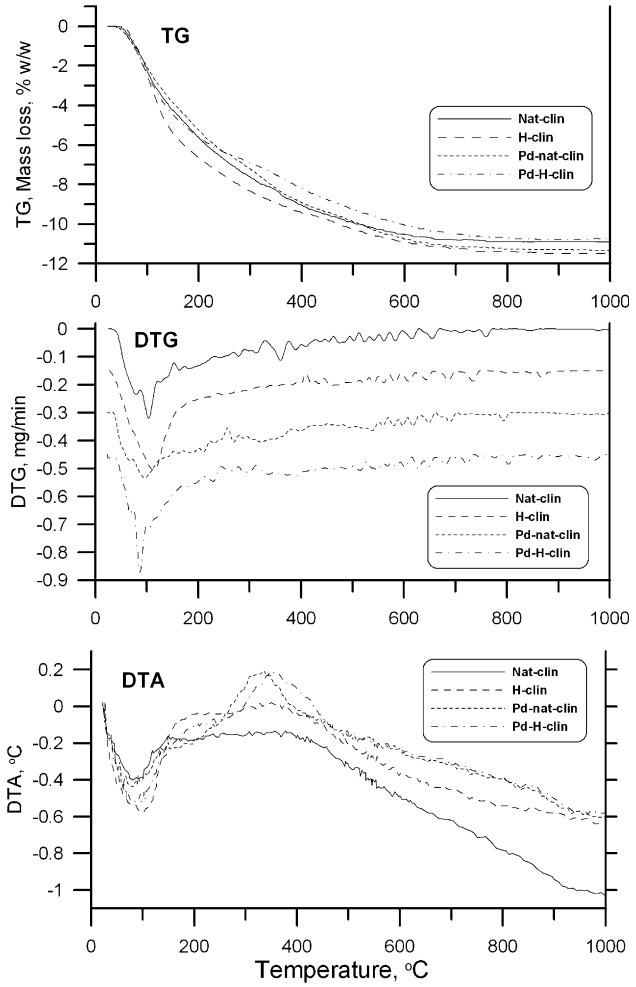

Fig. 10. TG, DTG and DTA curves of the different forms of clinoptilolite.

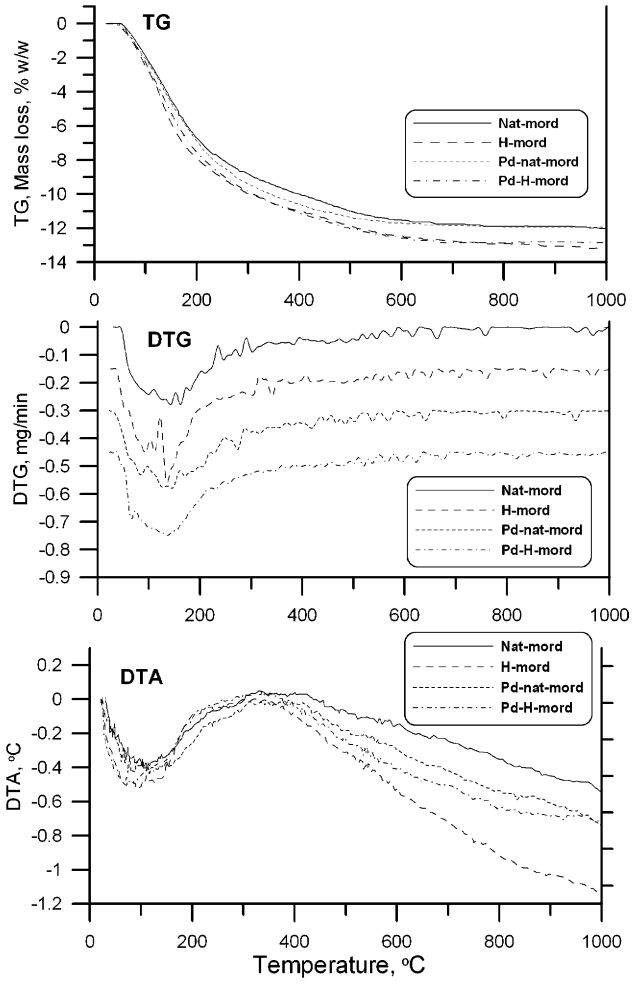

Fig. 11. TG, DTG and DTA curves of the different forms of mordenite.

thermal treatment, except of fluctuations of the water loss in certain temperature regions. The most essential loss of mass is observed at 100–200 °C and 200–400 °C because of desorption of intact water and associatively desorption of hydroxy species.

4. Conclusion

As follows from nitrogen adsorption/desorption isotherms and the pore size distributions, natural zeolites change the channel structure with different treatments because of increase in micropores contribution. All the studied sorbents are geometrically heterogeneous and possess broad pore size distributions with characteristic three narrow ($R < 2$ nm), narrow ($2 < R < 5$ nm) and broad ($R > 5$ nm) domains. Natural clinoptilolite and mordenite are characterized by small specific surface areas increasing significantly after modification. Natural zeolite samples do not possess micropores which, however, are observed for the hydrogen forms. The mesopore structure does not

Table 3
The results of thermal analysis of zeolite samples

Sample	Loss of mass (%, w/w)					Range of positive DTA peak T_{exo}, °C	T_{max}, °C	Range of negative DTA peak T_{endo}, °C	T_{min}, °C
	25–100	100–200	200–400	400–800	800–1000				
Nat-clin	2.2	3.4	3.4	1.9	0.01	–	–	36–150	88
H-clin	2.5	4.1	2.3	1.9	0.1	–	–	25–202	102
Pd–nat-clin	2.1	3.2	3.7	2.4	0.06	184–440	335	27–155	79
Pd–H-clin	2.4	3.2	2.6	2.5	0.07	277–451	355	30–207	82
Nat-mord	1.9	4.7	3.2	1.9	0.1	–	–	36–271	105
H-mord	2.5	5.2	3.2	1.9	0.3	–	–	30–198	94
Pd–nat-mord	2.0	4.8	3.7	1.4	0.1	–	–	30–224	114
Pd–H-mord	2.2	5.2	3.5	1.7	0.02	–	–	24–213	88

change with palladium sorption because only narrow pores are sensitive to its adsorption.

X-ray examination of the zeolite samples showed that acid treatment of both zeolites does not lead to significant structural changes. The analysis indicates increase in the amorphism of H-form of both zeolites and also heterogeneity of the sorbent composition. Appearance of peak at $2\theta = 26.84°$ and increasing peak intensity at $2\theta = 28.31°$ can be connected with palladium presence in the mordenite samples.

As follows from the FTIR photoacoustic study no new peaks appear on H-forms, which indicate insignificant changes in the surface structure due to its modification. However, there is a small displacement ($\Delta\nu = 10\ \mathrm{cm}^{-1}$) of band at $\nu = 1061\ \mathrm{cm}^{-1}$ for H-clin compared to Nat-clin, which can indicate elution of a small portion of Al^{3+} during acid treatment. For Pd-containing clinoptilolite, the ammonia band is at $1449\ \mathrm{cm}^{-1}$ which can be connected with both sorbed ammonia complexes with palladium and due to its interaction with surface hydroxy species.

The thermogravimetric analysis shows the presence of various types of intact water and surface hydroxy species. For H-form of both sorbents the elimination of greater amounts of physically bonded water is observed up to 120 °C. For Pd-containing clinoptilolite, the DTA curves have distinct exothermic peaks associated with desorption of ammonia complexes. In the case of mordenite, similar peaks are not observed because sorption proceeded in the nitrate medium.

Based on the studies it can be stated that the zeolite skeleton does not change on acidic processing but pores and channels change as a result of cations exchanging. These changes are more visible in the case of clinoptilolite.

Acknowledgment

This work was partially financed by the Ministry of education of Ukraine. R. Leboda is very grateful to the Foundation for Polish Science for financial support.

References

[1] E. Chmielewska-Chorvatova, J. Leśny, J. Radioanal. Nucl. Chem. Lett. 201 (1995) 293.
[2] G.V. Chcichishvili, T.G. Androkashvili, G.N. Kirov, L.D. Filizova, Natural Zeolites (in Russian), Khimia, Moscow, 1885.
[3] G. Yuan, H. Seyama, M. Soma, B.K.G. Theng, A. Tanaka, J. Environ. Sci. Health A 34 (3) (1999) 625.
[4] T. Liang, Appl. Radiat. Isot. 51 (1999) 527.
[5] S.K. Ouki, M. Kavannagh, Water Sci. Technol. 39 (1999) 115.
[6] D. Caputo, B. De Gennaro, M. Pansini, C. Colella, Porous Mater. Environ. Friendly Process. 125 (1999) 723.
[7] A. Langella, M. Pansini, P. Cappelletti, B. De Gennaro, M. De Gennaro, M. Colella, Micropor. Mesopor. Mater. 37 (2000) 337.
[8] A.A. Zorpas, T. Constantinides, A.G. Vlyssides, I. Haralambous, M. Loizidou, Bioresour. Technol. 72 (2000) 113.
[9] D. Feng, C. Aldrich, H. Tan, Hydrometallurgy 56 (2000) 359.
[10] M.I. Panayatova, Waste Manage. 21 (2001) 671.
[11] V.O. Vasylechko, L.O. Lebedynets, G.V. Gryshchouk, Yu.B. Kuz'ma, L.O. Vasylechko, T.M. Bernats'ka, Adsorp. Sci. Technol. 14 (1996) 267.
[12] V.O. Vasylechko, L.O. Lebedynets, G.V. Gryshchouk, R. Leboda, J. Skubiszewska-Zięba, Ochrona Orodowiska (Wroc3aw) 70 (1998) 3.
[13] V.O. Vasylechko, L.O. Lebedynets, G.V. Gryshchouk, R. Leboda, J. Skubiszewska-Zięba, Chem. Anal. (Warsaw) 44 (1999) 1013.
[14] V.O. Vasylechko, G.V. Gryshchouk, L.O. Lebedynets, Yu.B. Kuz'ma, L.O. Vasylechko, V.P. Zakordonskiy, Adsorp. Sci. Technol. 17 (1999) 125.
[15] V. Gomonaj, P. Gomonaj, N. Golub, K. Szekeresh, B. Charmas, R. Leboda, Adsorp. Sci. Technol. 18 (2000) 295.
[16] V.O. Vasylechko, G.V. Gryshchouk, Yu.B. Kuz'ma, L.O. Lebedynets, O.Ya. Oliyarnyk, Adsorp. Sci. Technol. 18 (2000) 621.
[17] V. Vasylechko, L. Lebedynets, Yu. Kuz'ma, G. Gryshchouk, V. Zakordonskiy, O. Karpyuk, Visnyk Lviv Univ. Ser. Khim. 39 (2000) 222.
[18] V.I. Gomonaj, N.P. Golub, K.Yu. Szekeresh, P.V. Gomonaj, B. Charmas, R. Leboda, Adsorp. Sci. Technol. 19 (2001) 465.
[19] V.O. Vasylechko, L.O. Lebedynets, G.V. Gryshchouk, Yu.B. Kuz'ma, L.O. Vasylechko, V.P. Zakordonskiy, in: A. Galarneau, F. Di Renzo, F. Fajula, J. Vedrine (Eds.), Zeolites and mesoporous materials at the dawn of the 21st century, Stud. Surf. Sci. Catal. Part C 135 (2001) 13.
[20] V.O. Vasylechko, G.V. Gryshchouk, Yu.B. Kuz'ma, V.P. Zakordonskiy, L.O. Vasylechko, L.O. Lebedynets, M.B. Kalytovs'ka, Micropor. Mesopor. Mater. 60 (2003) 183.
[21] E.J. Sullivan, D.B. Hunter, R.S. Bowman, Environ. Sci. Technol. 32 (1998) 1948.
[22] C. Díaz-Nava, M.T. Olguín, M. Solache-Ríos, Sep. Sci. Technol. 37 (13) (2002) 3109.
[23] M. Rivera-Garza, M.T. Olguín, I. García-Sosa, D. Alcántara, G. Rodríguez-Fuentes, Micropor. Mesopor. Mater. 39 (2000) 431.
[24] H.G. Karge, H.K. Beyer, Stud. Surf. Sci. Catal. 69 (1991) 43.
[25] T. Enhold, M. Sychrev, I.M. Astrelin, M. Rozwadowski, R. Gołębiewski, in: M. Rozwadowski (Ed.), Third Polish-Germany Zeolite Colloquium, Proceedings, Toruń, Poland, April 3–5, 1997, Nicola Copernicus University Press, Toruń, 1998, pp. 137–149.
[26] M. Sychev, R.A. van Santen, in: M. Rozwadowski (Ed.), Third Polish-Germany Zeolite Colloquium, Proceedings, Toruń, Poland, April 3–5, 1997, Nicola Copernicus University press, Toruń, 1998, pp. 225–238.
[27] M. Dams, L. Drijkoningen, B. Pauwels, G. Van Tendeloo, D.E. De Vos, P.A. Jacobs, J. Catal. 209 (2002) 225.
[28] A.W. Aylor, L.J. Lobree, J.A. Reimer, A.T. Bell, J. Catal. 172 (1997) 453.
[29] T.Ya. Vrublevs'ka, L.V. Vrons'ka, O.Ya. Korkuna, N.M. Matviychouk, Adsorp. Sci. Technol. 17 (1999) 29.
[30] T. Vrublevs'ka, O. Korkuna, Visnyk Nat. Univ. "L'vivska Politekchnika". Chem. Technol. Sub. Appl. 395 (2000) 100.
[31] O. Korkuna, T. Vrublevs'ka, Visnyk Lviv Univ. Ser. Khim. 41 (2002) 134.
[32] T. Vrublevs'ka, O. Korkuna, Chem. Anal. (Warsaw) 47 (2002) 945.
[33] T. Vrublevs'ka, O. Korkuna, Voprosy Khimii i Khimicheskoj Tekhnologii 9 (2003).
[34] Yu.I. Tarasevich, V.E. Polyakov, L.L. Badekha, Khim. Tekhnol. Vody 13 (1991) 132.
[35] F.M. Bobonich, A.A. Valter, Ya.V. Maslyakevich, Mineral. Zhurn. 90 (1980).
[36] C. Nguyen, D.D. Do, Langmuir 15 (1999) 3608.
[37] C. Nguyen, D.D. Do, Langmuir 16 (2000) 7218.
[38] V.M. Gun'ko, D.J. Sheeran, S.M. Augustine, J.P. Blitz, J. Colloid Interf. Sci. 249 (2002) 123.
[39] V.M. Gun'ko, J. Skubiszewska-Zięba, R. Leboda, K.N. Khomenko, O.A. Kazakova, M.O. Povazhnyak, I.F. Mironyuk, J. Colloid Interf. Sci. 269 (2004) 403.

[40] V.M. Gun'ko, V.V. Turov, J. Skubiszewska-Zięba, B. Charmas, R. Leboda, Adsorption 10 (2004) 5.
[41] S.W. Provencher, Comp. Phys. Commun. 27 (1982) 213.
[42] M.A. Hernández, Adsorption 6 (2000) 33.
[43] M.A. Hernández, J. Porous Mater. 7 (2000) 443.
[44] E.J. Sullivan, D.B. Hunter, R.S. Bowman, Clays Clay Miner. 45 (1997) 42.
[45] V.I. Starosta, Y.V. Voroshylov, B.M. Yershov, D.I. Melnyk, Naukovyj Visnyk UzhDU, ser. ''Khimija'' 2 (1997) 120.
[46] M.W. Kasture, P.N. Joshi, H.S. Soni, V.V. Joshi, A.L. Choudhari, V.P. Shiralkar, Adsorp. Sci. Technol. 16 (1998) 135.
[47] W. Mozgawa, J. Mol. Struct. 555 (2000) 299.
[48] M. Guisnet, P. Ayrault, J. Datka, Pol. J. Chem. 71 (1997) 1455.